

Sinogram constrained TV-minimization for metal artifact reduction in CT

Clemens Schiffer*and Kristian Bredies†

Abstract. A new method for reducing metal artifacts in X-ray computed tomography (CT) images is presented. It bases on the solution of a convex optimization problem with inequality constraints on the sinogram, and total variation regularization for the reconstructed image. The Chambolle-Pock algorithm is used to numerically solve the discretized version of the optimization problem. As proof of concept we present and discuss numerical results for synthetic data.

1 Introduction

X-ray computed tomography (CT) has become a major tool in medical imaging, yet metal inclusions in the patient, such as pacemakers, screws, orthopedic implants and dental fillings, still pose a problem. The basic principle of CT is rotating an X-ray source and an opposing detector around the object to be scanned, producing projection data from a range of angles. These projections of intensities, known as the sinogram, have to be reconstructed into a spatial image, in order to obtain the desired cross-section. To achieve this, the standard method is filtered back projection (FBP), which works very well under ideal or even normal circumstances. Still errors from various sources, such as patient movement, beam scatter etc. disturb this reconstruction process and lead to artifacts. In particular, the presence of metal inclusions produces significant dark and bright smears, known as metal artifacts, that may render the image unusable for diagnostics.

Existing techniques for reducing metal artifacts can be categorized into technical enhancements and computational methods. The former include the use of dual energy CT devices [1], which feature two sources that produce projections from different angles. The different energy levels used by the two sources allow to identify a substance by their specific absorption spectrum, this information can then be used to reduce metal artifacts. In contrast, computational methods focus on processing the already collected data in a way that removes the artifacts. This is, for instance, accomplished by replacing the corrupted data either in the spatial or the projection domain, e. g., by interpolation [10] or inpainting [5], with various refinements such as repeated projection, back-projection and replacement of bad data [2, 7]. Variational methods involving total variation regularization have been proposed [8], and applied with the recently developed Chambolle-Pock algorithm [9]. The novelty of our method lies in the dedicated treatment of metal artifacts by introducing pointwise inequality constraints on the sinogram in addition to total variation regularization of the image.

*Institute for Mathematics and Scientific Computing, University of Graz, Heinrichstraße 36, A-8010 Graz, Austria (clemens.schiffer@edu.uni-graz.at)

†Institute for Mathematics and Scientific Computing, University of Graz, Heinrichstraße 36, A-8010 Graz, Austria (kristian.bredies@uni-graz.at)

In Section 2 the problem is presented and mathematically modeled, in Section 3 the numerical solution is discussed and an algorithm for solving the proposed optimization problem is described, in Section 4 results are presented and, finally, in Section 5, a conclusion is given.

2 Problem and Mathematical Model

The object to be scanned is modeled as a continuous function $f(x, y)$ in \mathbb{R}^2 , that represents the density of the object at a point (x, y) . It is assumed to be zero outside a region of interest. The assumption of the model is that the attenuation an X-ray suffers, i. e. the loss of intensity, is proportional to the traversed density. Therefore, the process of an X-ray passing through the object, being weakened and received by a detector is modeled as integrating f over a straight line L

$$(Af)(\varphi, s) = \int_L f(x) ds, \quad (1)$$

where φ is the gradient angle of L and s its signed distance from the origin, the *offset*. This is called the *Radon transform* and the data it produces a *sinogram*, which is commonly interpreted as a function of angle and offset. Consider a ray that starts at the source with intensity $I(x_S)$ and whose intensity is measured at the detector giving $I(x_D)$. By the modeling assumption [6] we get

$$(Af)(\varphi, s) = \int_L f(x) ds = -\log(I(x_D)) + \log(I(x_S)). \quad (2)$$

Now if the ray passes through a very dense area, and is attenuated so strongly that the detector cannot differentiate its signal from noise, i. e. the received signal is unknown but lower than a certain threshold ε , then $I(x_D) < \varepsilon$. The intensity at the source $I(x_S)$ is considered constant, and therefore, we get $(Af)(\varphi, s) > -\log(\varepsilon) + \log(I(x_S)) =: C$. Thus, this process of beam cancellation is represented by “capping” the sinogram, i. e. defining a certain threshold C and considering the values for each point in the sinogram that exceeds C as unknown, but at least as great as the threshold. The domain of the sinogram is denoted as Ω , while the portion where the threshold is exceeded is denoted as Ω_0 . The capped sinogram is called U_0 and considered to be the given data. It is assumed - as in total variation denoising - that f has a certain spatial structure for the propose of this paper it is assumed to be piecewise constant and therefore to admit a low total variation semi-norm. In trying to reconstruct f we therefore look for an approximation u that has also low TV-norm and for which an application of the Radon transform will produce a sinogram that is similar to that of f in $\Omega \setminus \Omega_0$ and also has values greater or equal than C in Ω_0 . This leads to the optimization problem

$$\begin{cases} \min_{u \in X} & \frac{1}{2} \|Au - U_0\|^2 + \lambda \|\nabla u\|_1 \\ \text{s.t.} & Au|_{\Omega_0} \geq C \end{cases} \quad (3)$$

where $\|\cdot\| = \|\cdot\|_{L^2(\Omega \setminus \Omega_0)}$ and $\|\cdot\|_1 = \|\cdot\|_{L^1(\Omega)}$. Here $\lambda > 0$ serves as a balancing parameter between regularization via the total variation semi-norm, and the discrepancy between Au and U_0 , which is measured on $\Omega \setminus \Omega_0$ i. e. only on sinogram data that is considered to be correct. Using the indicator function

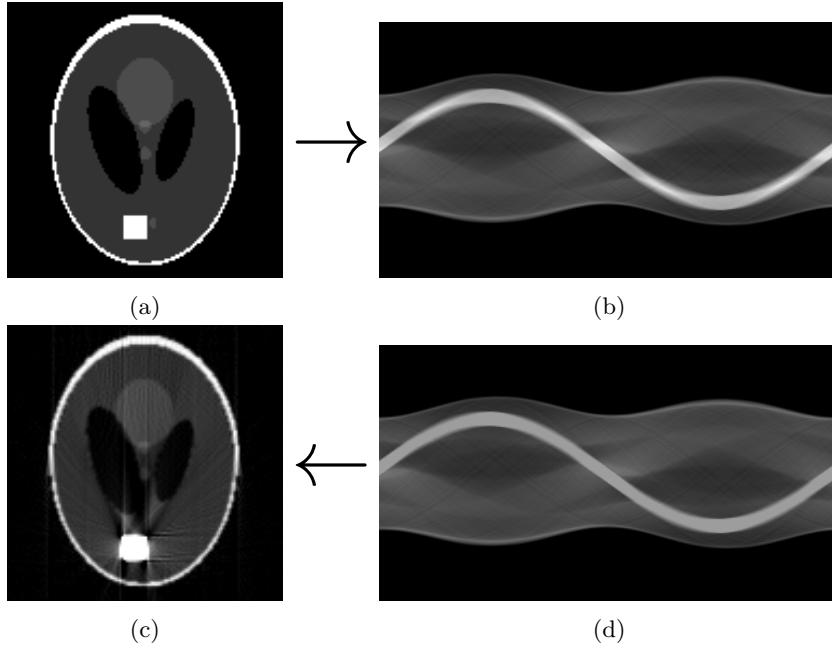


Figure 1: Metal artifacts are simulated with a synthetic test image. (a) shows a Shepp-Logan phantom, with values in $[0, 1]$ to which a block of value 3 has been added, simulating metal. (b) shows the result of applying the Radon transform, i. e. the corresponding sinogram. In (d), this sinogram has been capped: values greater than 45 have been set to 45, (c) shows the devastating results of simply applying the MATLAB-function *iradon* to the capped sinogram. Figures (a) and (c) display only values in $[0, 1]$ for better contrast.

$$I_M(x) = \begin{cases} 0, & \text{if } x \in M \\ \infty, & \text{if } x \notin M \end{cases} \quad (4)$$

where $0 \cdot \infty = 0$ and $1 \cdot \infty = \infty$ are set, we can reformulate (3) as

$$\min_{u \in X} \frac{1}{2} \|Au - U_0\|^2 + \lambda \|\nabla u\|_1 + I_{\{Au|_{\Omega_0} \geq C\}}(u). \quad (5)$$

The parameter λ is not needed if one enforces $Au = U_0$ in $\Omega \setminus \Omega_0$ as a hard constraint. Then, the minimization problem becomes

$$\begin{cases} \min_{u \in X} \|\nabla u\|_1 \\ \text{s.t. } Au|_{\Omega_0} \geq C \wedge Au|_{\Omega \setminus \Omega_0} = U_0 \end{cases} \quad (6)$$

which is equivalent to

$$\min_{u \in X} \|\nabla u\|_1 + I_{\{Au|_{\Omega_0} \geq C\}}(u) + I_{\{Au|_{\Omega \setminus \Omega_0} = U_0\}}(u). \quad (7)$$

3 Numerical Solution

We are numerically solving a discretized version of (5) and (7), following the presentation in [3]. In order to discretize the gradient ∇ a finite difference scheme with spacing h and zero boundary extension is used. Note that then, $\|\nabla_h\|^2 < \frac{8}{h^2}$ and its adjoint is $\nabla_h^* = -\text{div}_h$ with a similar discretization. The discretization of the Radon transform A_h is implemented as follows: Every point in the image domain is, for each of the N angles, projected onto the detector line, which is separated into M bins. The value at the point is then assigned proportionally to the two bins the point is projected inbetween. This implementation yields the same results as the MATLAB-function *radon*, when using 2×2 oversampling. The adjoint of the discrete Radon transform A_h^* is a discretization of the linear back projection, which is implemented similarly, each point in the image domain is projected onto the detector line and linear interpolation is performed. Then the values for all angles are summed up. Numerical tests confirm that this implementation provides the adjoint to the discrete Radon transform.

The optimization problems (5) and (7) are of the form

$$\min_{u \in X} F(u) + G(Ku), \quad (8)$$

with $F: X \rightarrow \mathbb{R}, G: Y \rightarrow \mathbb{R}$ convex, lower semi-continuous and proper, as well as $K: X \rightarrow Y$ linear and continuous. These problems satisfy the sufficient conditions for the Fenchel-Rockafellar duality [3]. The dual problem reads as

$$\max_{w \in Y^*} -F^*(-K^*w) - G^*(w). \quad (9)$$

Now, solving the primal and dual equation simultaneously can be interpreted as finding the saddle-point of the function

$$L(u, w) = \langle w, Ku \rangle + F(u) - G^*(w). \quad (10)$$

In order to solve this problem, the Chambolle-Pock algorithm [4]

$$\begin{cases} w^{k+1} = (id + \tau \partial G^*)^{-1}(w^k + \tau K \bar{u}^k) \\ u^{k+1} = (id + \sigma \partial F)^{-1}(u^k - \sigma K^* w^{k+1}) \\ \bar{u}^{n+1} = 2u^{k+1} - u^k \end{cases} \quad (11)$$

is employed, which converges to a saddle point of (10), if $\sigma\tau\|K\|^2 < 1$. In order to match the form of (8), the following discrete version of (3)

$$\min_{u \in \mathbb{R}^{n \times m}} \frac{1}{2} \|A_h u - U_0\|^2 + \lambda \|\nabla_h u\|_1 + I_{\{A_h u|_{\Omega_0} \geq C\}}(u) \quad (12)$$

is dualized with $F = 0$ and $G: \mathbb{R}^{N \times M} \times \mathbb{R}^{n \times m \times 2} \rightarrow \mathbb{R}_\infty$ as well as the linear mapping $K: \mathbb{R}^{m \times n} \rightarrow \mathbb{R}^{M \times N} \times \mathbb{R}^{m \times n \times 2}$ defined by

$$G(x, y) = \frac{1}{2} \|x - U_0\|^2 + I_{\{x|_{\Omega_0} \geq C\}}(x) + \lambda \|y\|_1 \quad K = \begin{bmatrix} A_h \\ \nabla_h \end{bmatrix}. \quad (13)$$

For $F = 0$ the resolvent is $(id + \sigma \partial F)^{-1} = id$, as for G^* its resolvent can be evaluated componentwise, i. e. for $G(x, y) = G_1(x) + G_2(y)$ we have

$$(id + \sigma \partial G^*)^{-1}(\bar{v}, \bar{w}) = \begin{pmatrix} (id + \sigma \partial G_1^*)^{-1}(\bar{v}) \\ (id + \sigma \partial G_2^*)^{-1}(\bar{w}) \end{pmatrix} \quad (14)$$

As $G_1(x) = \sum_{(i,j) \in \Omega \setminus \Omega_0} (x - U_0)_{i,j}^2 + \sum_{(i,j) \in \Omega_0} I_{x \geq C}(x_{i,j})$, its dual is

$$G_1^*(\xi) = \sum_{(i,j) \in \Omega \setminus \Omega_0} g_1^*(\xi_{i,j}) + \sum_{(i,j) \in \Omega_0} \bar{g}_1^*(\xi_{i,j}) \quad (15)$$

with $g_1^*(\xi_{i,j}) = \frac{1}{2} \xi_{i,j}^2 + \xi_{i,j}(U_0)_{i,j}$ and

$$\bar{g}_1^*(\xi_{i,j}) = \begin{cases} \infty, & \text{if } \xi_{i,j} > 0 \\ \xi_{i,j}C, & \text{if } \xi_{i,j} \leq 0 \end{cases} \quad (16)$$

consequently the resolvent can be calculated to be

$$(id + \tau \partial G_1^*)^{-1}(\bar{v}_{i,j}) = \begin{cases} \frac{\bar{v}_{i,j} - \tau(U_0)_{i,j}}{1 + \tau}, & \text{if } (i, j) \in \Omega \setminus \Omega_0 \\ \min\{\bar{v}_{i,j} - \sigma C, 0\}, & \text{if } (i, j) \in \Omega_0. \end{cases} \quad (17)$$

The dual of $G_2(y) = \lambda \|y\|_1$ is $G_2^*(\eta) = I_{B_\lambda^\infty(0)}(\eta)$, where $B_\lambda^\infty(0)$ denotes the norm ball of radius λ around the origin in the maximum norm, consequently the resolvent of G_2^* is the projection onto $B_\lambda^\infty(0)$:

$$((id + \tau \partial G_2^*)^{-1}(\bar{w}))_{i,j} = \left(\mathcal{P}_{B_\lambda^\infty(0)}(\bar{w}) \right)_{i,j} = \frac{\bar{w}_{i,j}}{\max\{1, |\bar{w}_{i,j}|/\lambda\}}. \quad (18)$$

Then, the Chambolle-Pock iteration provides us with Algorithm 1.

Algorithm 1 Chambolle-Pock algorithm for minimizing (12)

Require: Input: $U_0 \in \mathbb{R}^{N \times M}, C > 0, \sigma > 0, \tau > 0, h > 0$

Require: $\sigma\tau < (\|A\|^2 + \frac{8}{h^2})^{-1}$

$\Omega_0 \leftarrow \{(i, j) \mid (U_0)_{i,j} \geq C\}$

for $k < k_{max}$ **do**

$\bar{w} \leftarrow w + \tau \nabla_h \bar{u}$

$w \leftarrow \mathcal{P}_{B_\lambda^\infty(0)}(\bar{w})$

$\bar{v} \leftarrow v + \tau A \bar{u}$

$v_{i,j} \leftarrow \begin{cases} \min\{\bar{v}_{i,j} - \sigma C, 0\}, & \text{if } (i, j) \in \Omega_0 \\ (\bar{v}_{i,j} - \tau(U_0)_{i,j}) / (1 + \tau), & \text{else} \end{cases}$

$u_{new} \leftarrow u + \sigma \operatorname{div}_h(w) - \sigma A^*(v)$

$\bar{u} \leftarrow 2u_{new} - u$

$u \leftarrow u_{new}$

end for

In the case of hard constraints we have $G_1 = I_{\{x|_{\Omega_0} \geq C\}} + I_{\{x|_{\Omega \setminus \Omega_0} = U_0\}}$ and the resolvent of G_1^* is again $(id + \sigma \partial G_1^*)^{-1}(\bar{v}_{i,j}) = \min\{\bar{v}_{i,j} - \sigma C, 0\}$ in Ω_0 and in $\Omega \setminus \Omega_0$ we have $(id + \sigma \partial G_1^*)^{-1}(\bar{v}_{i,j}) = \bar{v}_{i,j} - \sigma(U_0)_{i,j}$ finally we can choose $\lambda > 0$ arbitrarily e.g. $\lambda = 1$.

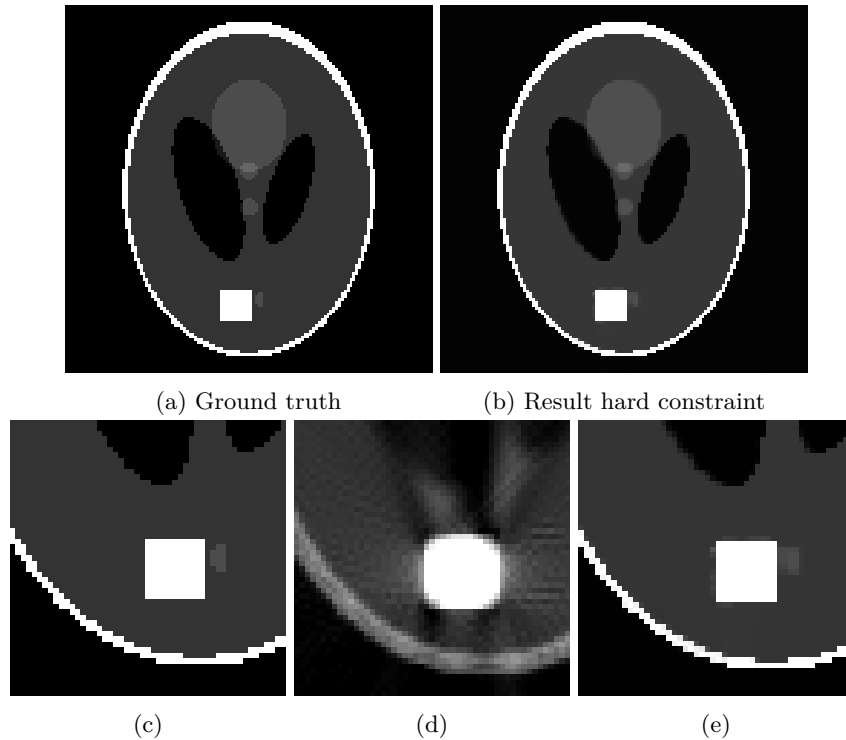


Figure 2: Results: (a) shows the ground truth again, (b) shows the result of the proposed method with hard constraints after 80000 iterations with Peak signal-to-noise ratio $\text{PSNR} = 47.6$ dB. In the second row details are shown, note the little area of tissue next to the metal in the ground truth (c), which along with other details is completely obscured in the reconstruction of the capped sinogram (d). In our result with hard constraints (e) the tissue next to the metal can at least be recognized, other details are preserved, but note the general blurriness.

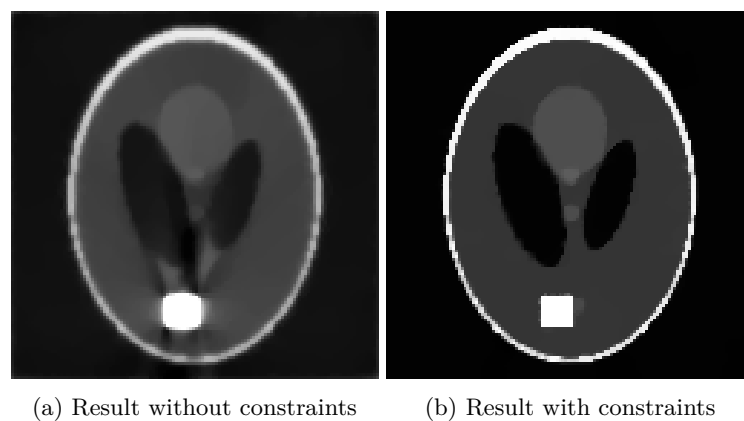


Figure 3: Results for reconstruction from a capped sinogram with 5% Gaussian noise, (a) shows the result of L2-TV minimization without constraints similar to the method presented in [9] if one does not account for the presence of metal, (b) shows the result of the proposed method of L2-TV minimization with constraints after 80000 iterations with Peak signal-to-noise ratio $\text{PSNR} = 40.1$ dB. The parameter $\lambda = 10^{-4.1}$ has been manually chosen, to optimize PSNR.

4 Experiments and Results

In order to test the proposed method, a Shepp-Logan phantom of size 128×128 pixels and values in $[0, 1]$ was used. In an area of 10×10 pixels the value 3 was added to representing a metallic object, see Figure 1(a). Applying the Radon transform results in the sinogram in Figure 1(b). Simply trying to reconstruct from the capped sinogram e. g. using the MATLAB[®] function *iradon* will result in artifacts (see Figure 1(c)) that are very similar to those seen in real reconstructions. Algorithm 1 was applied to the capped sinogram U_0 with the operator $A = \frac{1}{D} A_h$ where D is a crude bound for the norm of A_h . Then $\|A\| < 1$ and consequently, we used $\sigma = \tau < (1 + \frac{8}{h^2})^{-\frac{1}{2}}$, which led to a convergent algorithm. The result for hard constraints after 80000 iterations can be seen in Figure 2(b). Results for reconstruction the a capped sinogram with 5% Gaussian noise, using a L^2 data term after 80000 iterations can be seen in Figure 3(b), the parameter λ was manually chosen to optimize PSNR.

5 Discussion/Conclusion

A new method of reducing metal artifacts has been presented, and the results serve as a proof of concept, in particular the hard constrained optimization with synthetic data succeeds in removing the artifacts while preserving most of the details. The method is not limited to errors produced by metal, but could be extended to deal with any kind of corrupted or missing data. The most obvious drawback of the proposed method is the need for many iterations to produce satisfying results, which makes the method currently very slow. In our implementation this is mitigated to some extent by GPU-based parallelization, one iteration taking about 45 ms still leads to 80000 iteration on the toy problem taking about an hour, which prevents practical applications. We think that additional preconditioning may be necessary in order to provide adequate speed. We are optimistic that the method will also perform on more detailed and natural images without producing additional artifacts, and thus effectively and robustly remove metal artifacts in CT. A detailed study with respect to real data will be subject of future research.

References

- [1] Fabian Bamberg, Alexander Dierks, Konstantin Nikolaou, Maximilian F Reiser, Christoph R Becker, and Thorsten RC Johnson. Metal artifact reduction by dual energy computed tomography using monoenergetic extrapolation. *European radiology*, 21(7):1424–1429, 2011.
- [2] F Edward Boas and Dominik Fleischmann. Evaluation of two iterative techniques for reducing metal artifacts in computed tomography. *Radiology*, 259(3):894–902, 2011.
- [3] Kristian Bredies and Dirk Lorenz. *Mathematische Bildverarbeitung: Einführung in Grundlagen und moderne Theorie (German Edition)*. Vieweg+Teubner Verlag, 2010.
- [4] Antonin Chambolle and Thomas Pock. A first-order primal-dual algorithm for convex problems with applications to imaging. *Journal of Mathematical Imaging and Vision*, 40(1):120–145, 2011.

- [5] Yang Chen, Yinsheng Li, Hong Guo, Yining Hu, Limin Luo, Xindao Yin, Jianping Gu, and Christine Toumoulin. CT metal artifact reduction method based on improved image segmentation and sinogram in-painting. *Mathematical Problems in Engineering*, 2012, 2012.
- [6] Avinash C. Kak and Malcolm Slaney. *Principles of computerized tomographic imaging*. Society for Industrial and Applied Mathematics, 2001.
- [7] Seemeen Karimi, Pamela Cosman, Christoph Wald, and Harry Martz. Segmentation of artifacts and anatomy in CT metal artifact reduction. *Medical physics*, 39(10):5857–5868, 2012.
- [8] Ludwig Ritschl, Frank Bergner, Christof Fleischmann, and Marc Kachelrieß. Improved total variation-based CT image reconstruction applied to clinical data. *Physics in medicine and biology*, 56(6):1545, 2011.
- [9] Emil Y Sidky, Jakob H Jørgensen, and Xiaochuan Pan. Convex optimization problem prototyping for image reconstruction in computed tomography with the Chambolle–Pock algorithm. *Physics in medicine and biology*, 57(10):3065, 2012.
- [10] Yi Zhang, Yi-Fei Pu, Jin-Rong Hu, Yan Liu, Qing-Li Chen, and Ji-Liu Zhou. Efficient CT metal artifact reduction based on fractional-order curvature diffusion. *Computational and mathematical methods in medicine*, 2011, 2011.